INTERNATIONAL JOURNAL FOR NUMERICAL METHODS IN FLUIDS
Int. J. Numer. Meth. Fluids 2005; **47**:833–840
Published online 31 January 2005 in Wiley InterScience (www.interscience.wiley.com). DOI: 10.1002/fld.921

A ghost fluid, moving finite volume plus continuous remap method for compressible Euler flow

D. A. Bailey*,†, P. K. Sweby and P. Glaister

Department of Mathematics, The University of Reading, Whiteknights, PO Box 220, Berkshire, RG6 6AX Reading, U.K.

SUMMARY

A numerical solution method for accurately capturing material interfaces in unsteady compressible Euler flows is presented. The method consists of a finite volume scheme on a moving computational mesh and employs the HLLC approximate Riemann solver to evaluate intercell numerical fluxes. The mesh is moved in a Lagrangian fashion with the material, and to avoid grid distortion, remapping is performed at the end of each time interval, with the distorted grid being rezoned back to the initial mesh. The focus of the work is multimaterial flows consisting of two immiscible materials separated by an interface. The innovative aspect of the work is the application of a conservative ghost fluid method, together with a volume of fluid technique, within the moving mesh plus continuous remap framework. In addition a preliminary discussion, concerning the extension of the solution method to two spatial dimensions, includes a new area preserving volume fraction version of the interface reconstruction algorithm reported by Bonnell *et al.* (Material Interface Reconstruction. *Lawrence Livermore National Laboratory Report*). Copyright © 2005 John Wiley & Sons, Ltd.

KEY WORDS: moving finite volumes; ghost fluid; compressible Euler flows; material interface; continuous remap

1. GOVERNING EQUATIONS

In the reference frame of an arbitrary moving control volume, the Euler equations for one dimensional (1D), unsteady compressible flow, may be expressed in integral form as

$$\frac{\partial}{\partial t}\int_{\Omega(t)} \mathbf{q}(x,t)\,\mathrm{d}\Omega + \oint_{\Gamma(t)} \mathbf{f}(\mathbf{q}(x,t))\cdot\hat{n}\,\mathrm{d}\Gamma = 0 \tag{1}$$

The moving control volume $\Omega(t)$ is enclosed by its boundary $\Gamma(t)$, and $\hat{n}$ denotes the outward unit normal to $\Gamma(t)$. The vector of conserved variables is given by $\mathbf{q} = (\rho, \rho u, \rho E)^{\mathrm{T}}$, and the

*Correspondence to: D. A. Bailey, Department of Mathematics, The University of Reading, Whiteknights, PO Box 220, Berkshire, RG6 6AX Reading, U.K.
†E-mail: d.a.bailey@reading.ac.uk

Received 27 April 2004
Revised 17 December 2004
Accepted 19 December 2004

Copyright © 2005 John Wiley & Sons, Ltd.

flux vector is $\mathbf{f}(\mathbf{q}) = (u - \dot{x})\mathbf{q} + (0, p, up)^{\mathrm{T}}$, where ρ is density, u is flow velocity, $\dot{x}$ is the velocity of $\Gamma(t)$, E is specific total energy, and p is pressure. The system is completed by the ideal gas equation of state (EOS), $p = (\gamma - 1)\rho e$, where $e = E - \frac{1}{2}u$ is the specific internal energy and $\gamma\,(1 < \gamma < \frac{5}{3})$ is a constant representing the ratio of specific heat capacities of the material.

It is assumed that the flow consists of two immiscible components separated by a material interface. Each component is uniquely characterized by the value of γ in the EOS.

2. THE FINITE VOLUME SCHEME

The spatial domain is discretized into N non-overlapping computational cells, I_i, initially of a uniform size. The average value of $\mathbf{q}$ over each cell is approximated and stored at the cell centre (node). The governing equations (1) are discretized according to the conservative finite volume formula

$$\frac{\mathbf{Q}_i^{n+1}\Delta x_i^{n+1} - \mathbf{Q}_i^n \Delta x_i^n}{\Delta t} = -(\mathbf{F}_{i+1/2} - \mathbf{F}_{i-1/2}) \quad i = 0, \ldots, N \tag{2}$$

where

$$\mathbf{Q}_i^n \approx \frac{1}{\Delta x_i^n} \int_{x_{i-1/2}^n}^{x_{i+1/2}^n} \mathbf{q}(x, t^n)\,\mathrm{d}x \quad \text{and} \quad \mathbf{F}_{i-1/2} \approx \frac{1}{\Delta t} \int_{t^n}^{t^{n+1}} \mathbf{f}(\mathbf{q}(x_{i-1/2}(t), t))\,\mathrm{d}t \tag{3}$$

Here, Δx_i^n and $x_{i\pm1/2}^n$ are, respectively, the cell volume and cell boundaries at time t^n, and Δt is the variable time interval from time t^n to t^{n+1}. To evaluate $\mathbf{F}_{i-1/2}$ the cell average values are used to reconstruct a data distribution function in each cell of the domain, and the resulting Riemann problems that arise at the cell boundaries are solved approximately.

The mesh movement is determined by the evolution of the vertex positions. It is assumed that the vertex velocity $\dot{x}_{i-1/2}$ is constant in magnitude and direction during the time interval, and $\dot{x}_{i-1/2}$ is evaluated from the values of u^n using linear interpolation.

The size of the time step is evaluated, prior to each time interval, by selecting Δt to satisfy two constraints. The first constraint is that Δt should be chosen so that during a time interval none of the waves resulting from a Riemann problem travel more than half a cell width of the initial mesh. The second constraint is that Δt is chosen so that the mesh vertices are not displaced during the time interval by more than half a cell width of the initial mesh.

3. THE HLLC RIEMANN SOLVER

The principle behind the HLLC Riemann solver is to reduce the full Riemann problem to an approximate solution consisting of four constant states separated by three discontinuous waves. If the wave velocities of the three discontinuities are known, then application of the integral form of the conservation laws over an appropriate control volume, together with the assumption that particle velocity is constant within the internal structure of the Riemann solution, yields a closed form approximate expression for the intercell numerical flux.

Copyright © 2005 John Wiley & Sons, Ltd.

The original derivation [1] was with respect to a fixed reference frame. The expression below accounts for the movement of the mesh

$$\begin{aligned}\mathbf{F}^{\text{hllc}}_{i-1/2} = \tfrac{1}{2}[&(u_{\text{R}} - \dot{x}_{i-1/2})\mathbf{Q}_{\text{R}} + \mathbf{F}^{\text{lag}}_{K} + (u_{\text{L}} - \dot{x}_{i-1/2})\mathbf{Q}_{\text{L}} + \mathbf{F}^{\text{lag}}_{K} \\ &+ |S_{\text{L}} - \dot{x}_{i-1/2}|\mathbf{Q}_{\text{L}} - (|S_{\text{L}} - \dot{x}_{i-1/2}| - |S^{*} - \dot{x}_{i-1/2}|)\mathbf{Q}^{*}_{\text{L}} \\ &- |S_{\text{R}} - \dot{x}_{i-1/2}|\mathbf{Q}_{\text{R}} + (|S_{\text{R}} - \dot{x}_{i-1/2}| - |S^{*} - \dot{x}_{i-1/2}|)\mathbf{Q}^{*}_{\text{R}}]\end{aligned}$$

Here, $\mathbf{Q}_{\text{L}}$ and $\mathbf{Q}_{\text{R}}$ are, respectively, the left and right data states of the Riemann problem originating at $x^{n}_{i-1/2}$, $\mathbf{F}^{\text{lag}}_{K} = (0, p_K, u_K p_K)^{\text{T}}$ and $\mathbf{Q}^{*}_{K} = (\rho^{*}_{K}, \rho^{*}_{K} u^{*}_{K}, \rho^{*}_{K} E^{*}_{K})^{\text{T}}$ where $\rho^{*}_{K} = \rho_K(S_K - u_K)/(S_K - S^{*}), u^{*}_{K} = S^{*}, p^{*}_{K} = p_K + \rho_K(u_K - S_K)(u_K - S^{*})$ and $K = L, R$. The wave speed estimates S_{L}, S^{*} and S_{R} are acquired following an approach suggested in Reference [2].

A MUSCL–Hancock technique, involving characteristic slope limiting, is applied in order to obtain a high-resolution flux [1].

4. THE GHOST FLUID METHOD (GFM)

The material interface naturally divides the computational domain into two separate regions. Each point in the domain corresponds to one material or the other. In the GFM [3], ghost solution values (GSVs) are defined within the existing domain discretization in order to extend, each material region to the 'opposite' side of the interface. Hence, in a neighbourhood of the interface, each mesh node has associated with it, cell average values of mass, momentum and total energy for the real material in that cell, and ghost cell average values of mass, momentum and total energy for the material that does not really exist in that cell, but is located on the 'opposite side' of the interface. Once the GSVs are defined, the material regions are assumed separate identities, and each set of solution variables is evolved independently using the single material flow solver. The magnitude of the updated volume fractions are used to determine which of the two sets of solution variables is real at the new time level. GSVs are defined and discarded, respectively, at the beginning and end of the moving mesh phase of the proposed two-stage solution method. The one exception to this rule concerns the GSVs within the mixed cell. In order to be consistent with the remapping procedure and the conservative correction algorithm, the GSVs within the mixed cell are retained until the beginning of the next time interval. The process can be optimized for implementation by applying the method only in a band of cells on either side of the interface. An important feature of the GFM is that it regulates the complexities associated with the existence of multicomponent cells, whilst maintaining a Heaviside solution profile of density at the interface with no numerical diffusion or dispersion. There is no requirement to solve a multimaterial Riemann problem, consider the Rankine–Hugoniot jump conditions, or solve an IVP at the interface. Furthermore, there is freedom of choice concerning the single-component flow solver used with the method.

The success of the GFM relies on capturing the appropriate interface conditions when defining GSVs. Following the methodology of Reference [3], the pressure and velocity variables, which are continuous across the interface, are copied cell by cell into the GSVs from the real material (ensuring continuity of these variables). The remaining discontinuous variable, required to completely determine the flow solution, is extrapolated into the GSVs from a

Copyright © 2005 John Wiley & Sons, Ltd.

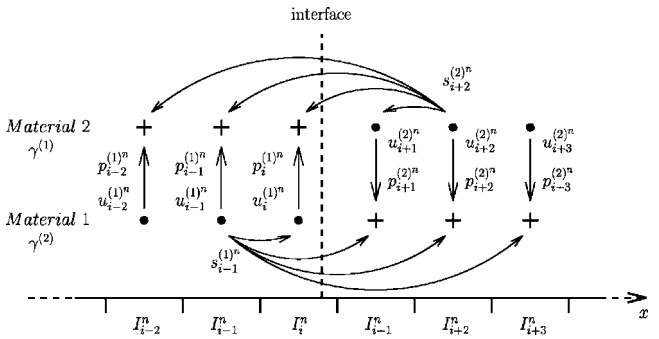

Figure 1. Defining GSVs using an isobaric fix. p is pressure, u is flow velocity and s is entropy.

reference state on the opposite side of the interface. In order to avoid numerical dissipation errors and associated spurious pressure oscillation phenomena, constant extrapolation is used, creating a continuous variable profile and minimizing the variation from the reference state. Based on work in Reference [4] and confirmed by numerical experiment, entropy is taken to be the extrapolated value. Figure 1 shows a schematic outlining the details involved in defining the GSVs. The figure also illustrates an isobaric fix being imposed. This involves using the extrapolation technique to alter the entropy values of the real material values near the interface, to further reduce numerical errors [3].

To obtain a fully conservative GFM, a post processing correction algorithm following on from work in Reference [5] is implemented in conjunction with the moving finite volume scheme.

The fractional volume, $\psi_i^{(M)}$, of each cell occupied by each material is stored. They are evolved in time independently of the flow solution according to a predictor–corrector discretization [6] of the equation

$$\frac{\partial \psi^{(M)}}{\partial t} + \frac{\partial}{\partial x}(\psi^{(M)}\dot{u}) = \frac{\psi^{(M)}\bar{K}_S}{\bar{\rho}K_S^{(M)}} \cdot \frac{\partial \dot{u}}{\partial x} \tag{4}$$

where $K_S = \gamma^{(M)} p^{(M)}$, $\bar{\rho} = \sum_{M=1}^{2} \psi^{(M)}\rho^{(M)}$, $\bar{K}_S = (\sum_{M=1}^{2} \psi^{(M)}/K_S^{(M)})^{-1}$ and $\dot{u}$ is the flow velocity relative to the moving reference frame. Equation (4) ensures adherence to the constraint $\sum_{M=1}^{2} \psi_i^{(M)} = 1$.

5. REMAPPING/REZONING

The remap procedure may be regarded as integrating the known solution variables on the old grid over the cell of a new mesh. In this work remapping is performed periodically at the end of each time step and the grid is rezoned to the initial uniform mesh. The actual quantities remapped are the conserved variables. In multi-material flows each material is rezoned separately and the values of the volume fractions are modified in accordance with

Copyright © 2005 John Wiley & Sons, Ltd.

the transfer of data from the old mesh to the new. The remap procedure for material M in cell I_i may be expressed in integral form as

$$\bar{\mathbf{Q}}_i^{(M)} = \frac{1}{\Delta \bar{x}_i} \int_{\bar{x}_{i-1/2}}^{\bar{x}_{i+1/2}} \tilde{\mathbf{Q}}^{(M)}(x, t^{n+1})\, \mathrm{d}x \tag{5}$$

The overbar denotes remapped values and $\tilde{\mathbf{Q}}(x, t^{n+1})$ is a data distribution function reconstructed from the cell average values $\mathbf{Q}_i^{n+1}$. Equation (5) can be evaluated as a sum of integrals over the intersection regions between cell $\bar{I}_i$ and the cells on the old distorted mesh [7]. The accuracy of the remap procedure is determined by the degree of $\tilde{\mathbf{Q}}$. Numerical experiment disclosed a pressure oscillation at the interface when remapping with a piecewise linear $\tilde{\mathbf{Q}}$ function. This phenomenon was eliminated by remapping with first-order accuracy in a neighbourhood of the interface, whilst maintaining higher-order accuracy throughout the remainder of the domain. The mesh is rezoned by returning it to the position it held at the beginning of the time interval. The remapping process is conservative. In terms of efficiency, remapping need only be implemented within areas of the computational domain where the mesh was displaced in the first phase of the proposed two-stage solution method.

6. 2D—PRELIMINARY DISCUSSION

Current work is proposing to extend the presented numerical method to two-dimensional, unsteady multimaterial compressible Euler flows. In this instance governing equations may be written in integral form as

$$\frac{\partial}{\partial t} \iint_{\Omega(t)} \mathbf{q}(x, y, t)\, \mathrm{d}\Omega + \oint_{\Gamma(t)} (\mathbf{f}(\mathbf{q}(x, y, t)), \mathbf{g}(\mathbf{q}(x, y, t))) \cdot \hat{n}\, \mathrm{d}\Gamma = 0 \tag{6}$$

where $\Omega(t)$ is the moving control volume enclosed by its boundary $\Gamma(t)$, $\mathbf{q} = (\rho, \rho u, \rho v, \rho E)$, $\mathbf{f}(\mathbf{q}) = (u - \dot{x})\mathbf{q} + (0, p, 0, up)$, $\mathbf{g}(\mathbf{q}) = (v - \dot{y})\mathbf{q} + (0, 0, p, vp)$, and $\hat{n}$ denotes the outward unit normal to $\Gamma(t)$. The system of equations (6) is discretized through the following dimensional splitting:

$$\mathbf{Q}_{i,j}^{n+1'} = \frac{\Omega_{i,j}^n}{\Omega_{i,j}^{n+1'}} \left(\mathbf{Q}_{i,j}^n - \frac{\Delta t}{\Omega_{i,j}^n} \left[s_{i+1/2,j}^n \mathbf{F}_{i+1/2,j} - s_{i-1/2,j}^n \mathbf{F}_{i-1/2,j} \right] \right), \quad \mathbf{F}_{i-1/2,j}(\mathbf{Q}_{i-1,j}^n, \mathbf{Q}_{i,j}^n, \bar{u}) \tag{7}$$

$$\mathbf{Q}_{i,j}^{n+1} = \frac{\Omega_{i,j}^{n+1'}}{\Omega_{i,j}^{n+1}} \left(\mathbf{Q}_{i,j}^{n+1'} - \frac{\Delta t}{\Omega_{i,j}^{n+1'}} \left[s_{i,j+1/2}^{n+1'} \mathbf{G}_{i,j+1/2} - s_{i,j-1/2}^{n+1'} \mathbf{G}_{i,j-1/2} \right] \right), \quad \mathbf{G}_{i,j-1/2}(\mathbf{Q}_{i,j-1}^{n+1'}, \mathbf{Q}_{i,j}^{n+1'}, \bar{v}) \tag{8}$$

where $\Omega_{i,j}^n$ is the volume of cell $I_{i,j}$ at time t^n, $\bar{u}, \bar{v}$, and $s_{i-1/2,j}, s_{i,j-1/2}$ are, respectively, facial velocities and lengths calculated in accordance with Reference [8]. $\mathbf{F}_{i-1/2,j}$ and $\mathbf{G}_{i,j-1/2}$ are numerical approximations to the time average flux across faces $\Gamma_{i-1/2,j}$ and $\Gamma_{i,j-1/2}$, respectively. They are evaluated by solving the x and y split one-dimensional Riemann problem using the HLLC Riemann solver in conjunction with the GFM. Evaluation of Δt takes into account wave speeds and mesh dimensions in both spatial directions.

Copyright © 2005 John Wiley & Sons, Ltd.

The principle of the GFM in 2D is the same as in 1D. However, in 2D defining the GSVs is more involved since there is more than one velocity component and a choice for the direction of extrapolation must be made. The GSVs for the pressure and velocity components are defined by setting them equal to the real material values in each cell in the computational domain. Constant extrapolation of entropy into cells containing and bordering the interface is performed in the direction of the normal to the interface. The normal value is extracted from a piecewise linear interface reconstructed from the fractional volume data.

The interface reconstruction algorithm develops an approach presented in Reference [9]. Reconstruction of a linear interface in an interface cell is transformed to a problem that analyses a 'local central dual' mesh of the interface cell in question and its eight surrounding cells. Each vertex in the dual mesh has associated with it the volume fraction of the cell within which it is centred. Material boundaries on the dual mesh are found by considering the volume fractions in 'material space' and evaluating intersections with Voronoi cells that represent the regions where one material dominates. These intersections are used to calculate interface points on the dual mesh. With a complete set of interface points on the dual mesh, the interface line, created through connection of the interface points, is transformed into a linear approximation to the interface within the original interface cell. The position of the interface line is adjusted to ensure the correct volume fraction is captured.

In 2D the remap procedure remains an integration problem, with each material being rezoned separately through integration over polygonal mesh overlap regions. At present a conservative correction algorithm has not been implemented with the 2D scheme, and the method is first-order accurate.

7. NUMERICAL RESULTS

In 1D, the selected test problem is a two material shock tube problem [10]. The initial conditions of the test consist of two constant states separated by a discontinuity. The two states are given by $(\rho_L, u_L, p_L)^T = (10, 50, 1.1 \times 10^5)^T$ and $(\rho_R, u_R, p_R)^T = (1, 50, 1 \times 10^5)^T$ with $\gamma_L = 1.4$

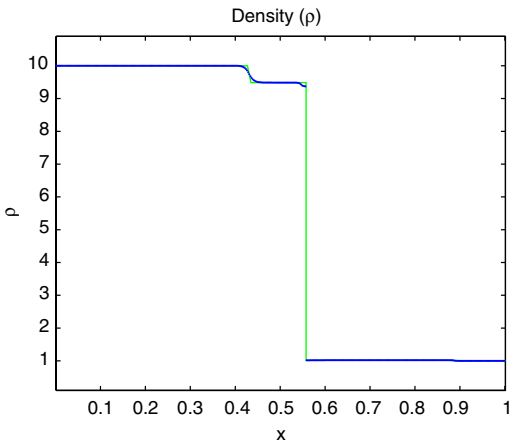

Figure 2. 1D density.

Copyright © 2005 John Wiley & Sons, Ltd.

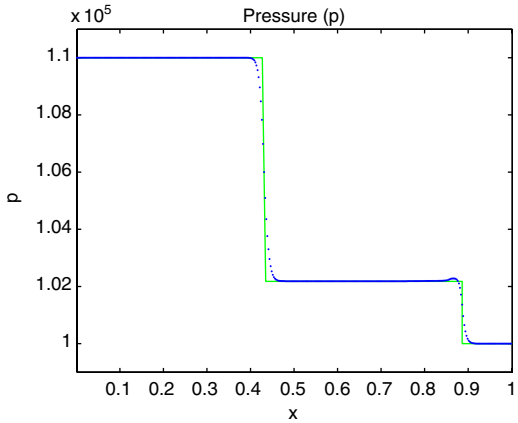

Figure 3. 1D pressure.

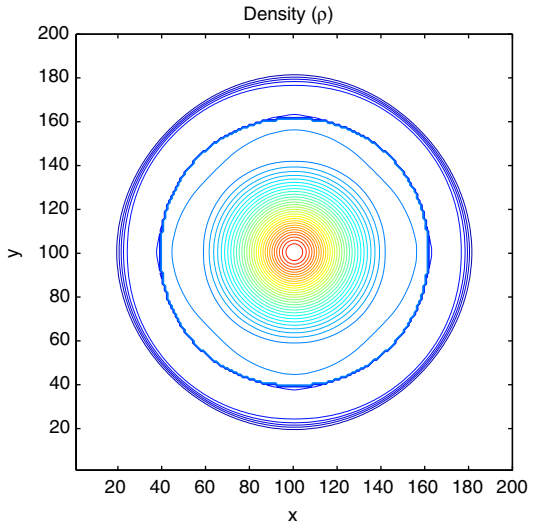

Figure 4. 2D density.

and $\gamma_R = 1.1$. The discontinuity was initially situated at $x = 0.505$. The numerical (dotted line) and exact (solid line) solutions are computed in the spatial domain [0,1] and the output time is $t = 0.001$ s. The numerical solution is computed with 400 cells and transmissive boundary conditions are applied. Figures 2 and 3 shows good agreement between the numerical and analytical solutions of density and pressure. The 2D test problem is a cylindrical explosion problem [1]. The governing equations are solved in the spatial domain $[0,2] \times [0,2]$. Initial conditions consist of a region inside a circle of radius 0.4 centred at (1,1), and the region outside of this circle. Initially, the flow variables take constant values in each of these regions, and are joined by a circular discontinuity. The two states are given by $(\rho_{in}, u_{in}, v_{in}, p_{in})^T = (1.0, 0.0, 0.0, 1.0)^T$

Copyright © 2005 John Wiley & Sons, Ltd.

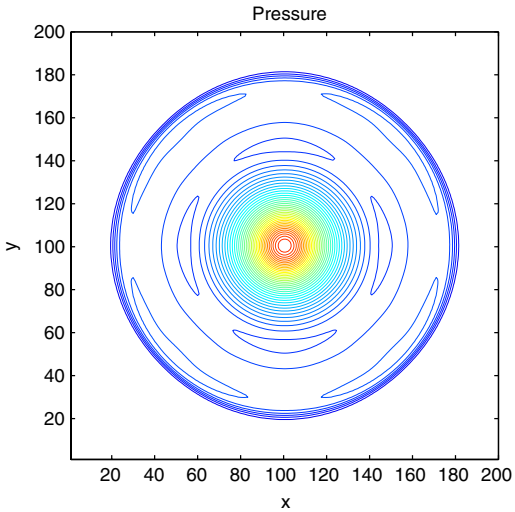

Figure 5. 2D pressure.

and $(\rho_{\text{out}}, u_{\text{out}}, v_{\text{out}}, p_{\text{out}})^{\text{T}} = (0.125, 0.0, 0.0, 0.1)^{\text{T}}$ with $\gamma_{\text{L}} = 1.6$ and $\gamma_{\text{R}} = 1.2$. The output time is $t = 0.25$ s. Results for density and pressure are shown, respectively, in Figures 4 and 5.

REFERENCES

1. Toro EF. *Riemann Solvers and Numerical Methods for Fluid Dynamics*. Springer: Berlin, 1997.
2. Batten P, Clarke N, Lambert C, Causon DM. On the choice of wavespeeds for the HLLC Riemann solver. *SIAM Journal on Scientific Computing* 1997; **18**(6):1553–1570.
3. Fedkiw RP, Aslam T, Merriman B, Osher S. A non-oscillatory Eulerian approach to interfaces in multimaterial flows (the ghost fluid method). *Journal of Computational Physics* 1999; **152**:457–492.
4. Fedkiw RP, Marquina A, Merriman B. An isobaric fix for the overheating problem in multimaterial compressible flows. *Journal of Computational Physics* 1999; **148**:545–578.
5. Nguyen D, Gibou F, Fedkiw R. A fully conservative ghost fluid method and stiff detonation waves. *12th International Detonation Symposium*, San Diego, CA, 2002.
6. Miller GH, Puckett EG. A high-order Godunov method for multiple condensed phases. *Journal of Computational Physics* 1996; **128**:134–164.
7. Sims P. Interface tracking using Lagrangian–Eulerian methods. *Thesis*, University of Reading, 1999.
8. Zhang H, Reggio M, Treepanier JY, Camarero R. Discrete form of the GCL for moving meshes and its implementation in CFD schemes. *Computers and Fluids* 1993; **22**:9–23.
9. Bonnell KS, Duchaineau MA, Schikore DR, Hamann B, Joy KI. Material interface reconstruction. *Lawrence Livermore National Laboratory Report*.
10. Barberon T, Helluy P, Rouy S. Practical computation of axisymmetrical multifluid flows. *International Journal of Finite Volumes* (*electronic*) 2003; **1**:1–34.

Copyright © 2005 John Wiley & Sons, Ltd.